RAPID COMMUNICATIONS

PHYSICAL REVIEW B **78**, 220510(R) (2008)

Evidence of nodeless superconductivity in $FeSe_{0.85}$ from a muon-spin-rotation study of the in-plane magnetic penetration depth

R. Khasanov,[1,*] K. Conder,[2] E. Pomjakushina,[2,3] A. Amato,[1] C. Baines,[1] Z. Bukowski,[4] J. Karpinski,[4] S. Katrych,[4] H.-H. Klauss,[5] H. Luetkens,[1] A. Shengelaya,[6] and N. D. Zhigadlo[4]

[1]*Laboratory for Muon Spin Spectroscopy, Paul Scherrer Institute, CH-5232 Villigen PSI, Switzerland*
[2]*Laboratory for Developments and Methods, Paul Scherrer Institute, CH-5232 Villigen PSI, Switzerland*
[3]*Laboratory for Neutron Scattering, Paul Scherrer Institute and ETH Zürich, CH-5232 Villigen PSI, Switzerland*
[4]*Laboratory for Solid State Physics, ETH Zürich, CH-8093 Zürich, Switzerland*
[5]*IFP, TU Dresden, D-01069 Dresden, Germany*
[6]*Physics Institute, Tbilisi State University, Chavchavadze 3, GE-0128 Tbilisi, Georgia*

(Received 9 October 2008; revised manuscript received 28 October 2008; published 31 December 2008)

The in-plane magnetic penetration depth λ_{ab} of the iron selenide superconductor with the nominal composition $FeSe_{0.85}$ was studied by means of muon-spin rotation. The measurements of $\lambda_{ab}^{-2}(T)$ are inconsistent with a simple isotropic s-wave type of the order parameter but are rather in favor of two-gap ($s+s$) and anisotropic s-wave order parameter symmetries, thus implying that the superconducting energy gap in $FeSe_{0.85}$ contains no nodes.

DOI: 10.1103/PhysRevB.78.220510 PACS number(s): 76.75.+i, 74.70.−b

The recent discovery of the Fe-based high-temperature superconductors has attracted considerable attention to the pnictides. Initially, superconductivity was found in $LaO_{1-x}F_xFeAs$ (Ref. 1) and, later on, in other single-layer pnictides by replacing La with various rare-earth elements (Ce, Pr, Nd, Sm, Gd, Tb, Dy, Ho, and Y) (Ref. 2) as well as in oxygen-free compounds such as doped double-layer MFe_2As_2 (M=Ba, Sr, and Ca) (Ref. 3) and single-layer LiFeAs.[4] The common structural feature of all these materials is the Fe-As layers consisting of an Fe square planar sheet tetrahedrally coordinated by As. Recently, superconductivity with the transition temperature $T_c \simeq 8$ K was discovered in α-FeSe with PbO structure.[5] This compound also has an Fe square lattice with Fe atoms tetrahedrally coordinated by Se ones [see Fig. 1(a)], similar to the structure of FeAs planes in the single- and the double-layer pnictides. In this respect FeSe, consisting of the "superconducting" Fe-Se layers only, can be treated as a prototype of the known families of Fe-As-based high-temperature superconductors and, consequently, becomes a good model system to study mechanisms leading to the occurrence of superconductivity in this class of materials.

Here we report a study of the in-plane magnetic field penetration depth λ_{ab} in iron selenide superconductor with the nominal composition $FeSe_{0.85}$ by means of muon-spin rotation (μSR). $\lambda_{ab}^{-2}(T)$ is reconstructed from the temperature dependences of the μSR linewidth measured at $\mu_0H=0.01$ T. The observed $\lambda_{ab}^{-2}(T)$ is found to be well described within the framework of anisotropic s-wave as well two-gap $s+s$-wave models. In a case of anisotropic s-wave model the maximum value of the gap at $T=0$ is $\Delta_0=2.24(1)$ meV leading to $2\Delta_0/k_BT_c=6.27(3)$. The two-gap $s+s$-wave model yields $\Delta_{0,1}=1.60(2)$ meV and $\Delta_{0,2}=0.38(1)$ meV. The corresponding gap to T_c ratios are $2\Delta_{0,1}/k_BT_c=4.49(6)$ and $2\Delta_{0,2}/k_BT_c=1.07(2)$ close to those reported for various single- and double-layer Fe-based superconductors.[6–8]

Details on the sample preparation for $FeSe_{0.85}$ can be found elsewhere.[5] X-ray diffraction analysis reveals that the α-FeSe phase is dominant and that the impurity fraction does not exceed $\simeq 7-10\%$. The ac and dc magnetization measurements were performed on Quantum Design physical property measurement system (PPMS) and magnetic property measurement system (MPMS) magnetometers at temperatures ranging from 1.75 to 300 K and magnetic fields between 0 and 6 T. The superconducting transition temperature T_c =8.26(2) K was obtained as an intersection of the linearly extrapolated ac magnetization curve [$M_{ac}(T)$] with M_{ac} =const line [see Fig. 1(b)]. dc magnetization (M_{dc}) experiments, conducted at $T=10$ and 150 K, suggest the presence of a sizeable amount of ferromagnetic fraction. M_{dc} saturates at $\mu_0H \gtrsim 1$ T to the value of $\sim 1.5\times10^5$ A/m [see Fig. 1(c)].

Zero-field (ZF), longitudinal-field (LF) and transverse-field (TF) μSR experiments were performed at the $\pi M3$

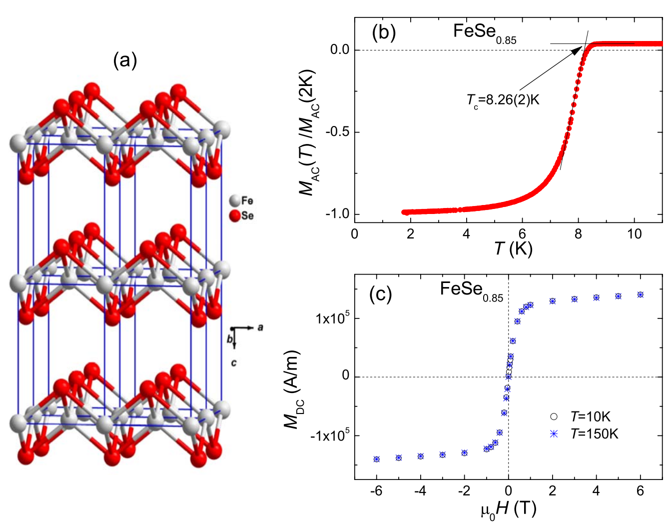

FIG. 1. (Color online) (a) The crystal structure of α-FeSe. (b) Temperature dependence of the ac magnetization M_{ac} (μ_0H_{ac} =0.1 mT and $\nu=1000$ Hz) of $FeSe_{0.85}$. (c) Dependence of dc magnetization M_{dc} on magnetic field at $T=10$ K and 150 K.

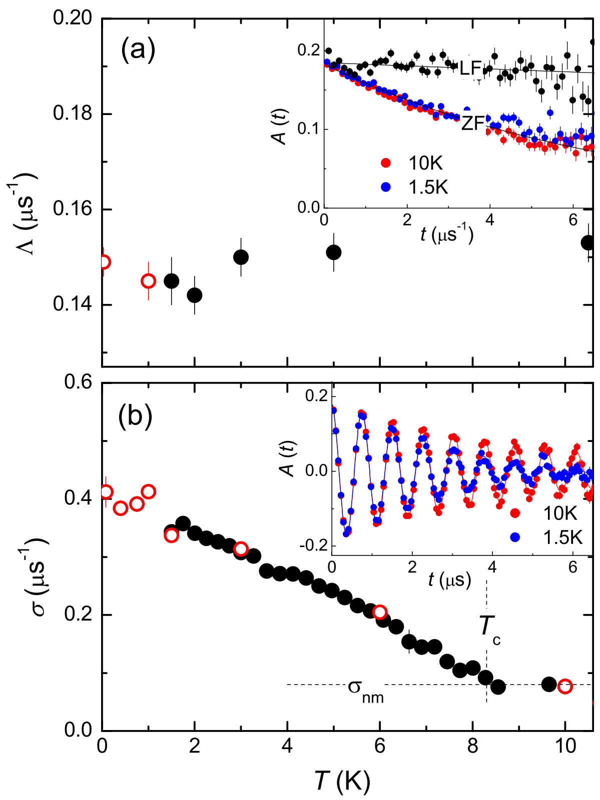

FIG. 2. (Color online) (a) Temperature dependence of the ZF muon depolarization rate Λ of $FeSe_{0.85}$. The inset shows ZF ($T=1.5$ and 10 K) and LF ($T=10$ K and $\mu_0 H=0.01$ T) μSR time spectra of $FeSe_{0.85}$. (b) Temperature dependence of the Gaussian depolarization rate σ obtained in TF μSR experiment at $\mu_0 H=0.01$ T. The inset shows the TF muon-time spectra above ($T=10$ K) and below ($T=1.5$ K) the superconducting transition temperature $T_c=8.26$ K.

beamline of the Paul Scherrer Institute (Villigen, Switzerland). Here LF and TF denote the cases when the magnetic field is applied parallel and perpendicular to the initial muon-spin polarization, respectively. The experiments down to $T\simeq 1.5$ K were performed on the low-background General Purpose Surface-Muon (GPS) instrument and those down to $T\simeq 0.02$ K on the Low-Temperature-Facility (LTF) instrument.

First we are going to present results of the ZF experiments. In the whole temperature region the ZF data were found to be well described by the single-exponential decay function

$$A^{ZF}(t)=A_0\exp(-\Lambda t). \quad (1)$$

Here A_0 is the initial asymmetry at $t=0$ and Λ is the exponential depolarization rate. The results of the analysis of the ZF data and the representative ZF and LF muon-time spectra are shown in Fig. 2(a). The open and the closed symbols are from the measurements taken on the LTF and the GPS instruments, respectively.

The exponential character of the muon polarization decay might be explained either by existence of fast electronic fluctuations measurable within the μSR time window[9] or by a static magnetic field distribution caused by diluted and randomly oriented magnetic moments.[10] To distinguish between these two cases LF μSR experiments were performed. As is shown in Ref. 11 in a case when the applied longitudinal field is much stronger than the internal one ($B>10B_{int}$) the muon spins become "decoupled" from the static internal field. On the other hand, field fluctuations perpendicular to the applied external field can cause irreversible spin-flip transitions of the muon spin, leading to depolarization.[9] As is shown in the inset of Fig. 2(a) an external field of 0.01 T is already enough to completely decouple the muon spins. This proves that the magnetism in $FeSe_{0.85}$ sample studied here is static in origin and is caused by diluted and randomly distributed magnetic moments. Bearing this in mind and by taking into account the presence of the relatively high paramagnetic contribution at $T>T_c$ [see Figs. 1(b) and 1(c)] we may conclude that the magnetism observed in both, ZF μSR and magnetization experiments, has similar sources and, most probably, caused by the traces of Fe impurities.[5]

The in-plane magnetic penetration depth λ_{ab} was studied in the TF μSR experiments. In a powder sample the magnetic penetration depth λ can be extracted from the Gaussian muon-spin depolarization rate $\sigma_{sc}(T)\propto 1/\lambda^2(T)$, which probes the second moment of the magnetic field distribution in the mixed state.[12] For highly anisotropic layered superconductors (such as the pnictide superconductors), λ is mainly determined by the in-plane penetration depth λ_{ab} (Ref. 13): $\sigma_{sc}(T)\propto 1/\lambda_{ab}^2(T)$. By taking into account the weak magnetism observed in ZF experiments [see Fig. 2(a) and discussion above], the TF μSR data were analyzed by using the following functional form:

$$A^{TF}(t)=A_0\exp(-\Lambda t)\exp(-\sigma^2 t^2/2)\cos(\gamma_\mu B_{int}t+\phi). \quad (2)$$

Here $\gamma_\mu/2\pi=135.5$ MHz/T is the muon gyromagnetic ratio, ϕ is the initial phase of the muon-spin ensemble, and $\sigma=(\sigma_{sc}^2+\sigma_{nm}^2)^{0.5}$ is the Gaussian relaxation rate. σ_{nm} is the nuclear magnetic dipolar contribution which is generally temperature independent.[14] The whole set of 0.01 T TF μSR data was fitted simultaneously with A_0, Λ, and ϕ as common parameters and σ and B_{int} as individual parameters for each temperature point. The exponential relaxation rate was assumed to be temperature independent in accordance with the results of our ZF μSR experiments [see Fig. 2(a)]. σ_{nm} was fixed to the value obtained above T_c where $\sigma=\sigma_{nm}$ [see Fig. 2(b)]. The results of the analysis and the representative TF muon-time spectra are shown in Fig. 2(a). The open and the closed symbols are again from the measurements taken on the LTF and the GPS instruments, respectively.

The superconducting part of the Gaussian depolarization rate σ_{sc} can be converted into λ_{ab} via[9,13,15]

$$\sigma_{sc}^2/\gamma_\mu^2=0.00126\ \Phi_0^2/\lambda_{ab}^4, \quad (3)$$

where $\Phi_0=2.068\times 10^{-15}$ Wb is the magnetic flux quantum. Figure 3 shows $\lambda_{ab}^{-2}(T)$ obtained from the measured $\sigma_{sc}(T)$ by means of Eq. (3). Regarding the pairing symmetry, available experimental results on various single- and double-layer Fe-based superconductors are divided between those favoring isotropic[16,17] as well as anisotropic[18,19] nodeless gaps and those supporting line nodes.[20] The two-gap behavior was

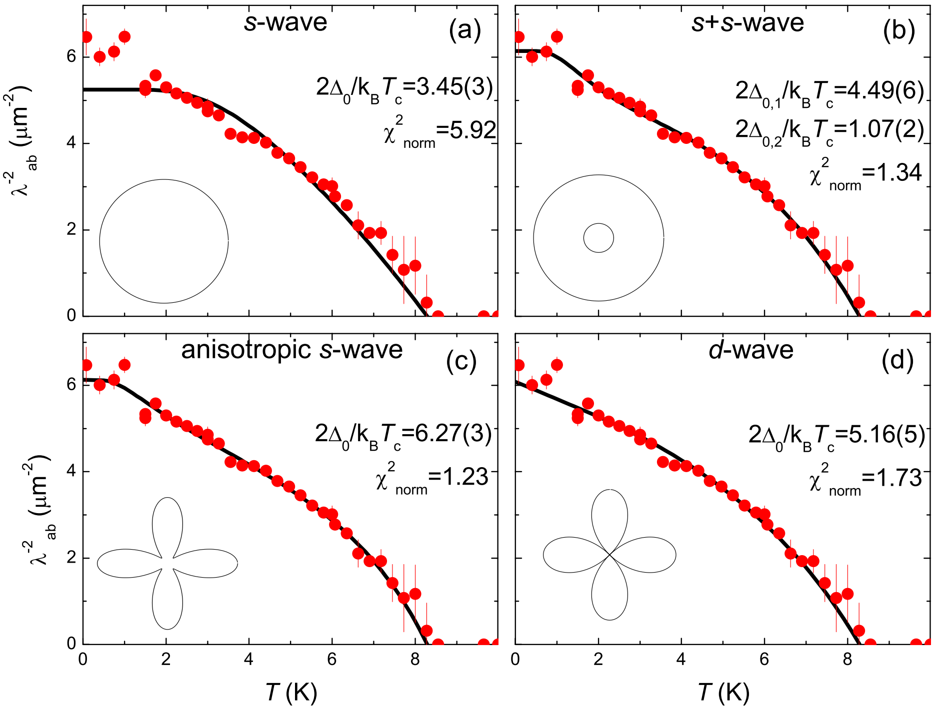

FIG. 3. (Color online) Temperature dependence of λ_{ab}^{-2} of $FeSe_{0.85}$ obtained from measured σ_{sc} by means of Eq. (3). The fitting curves (solid black lines) were obtained within the following models of the gap symmetries: (a) *s*-wave, (b) *s*+*s*-wave, (c) anisotropic *s*-wave, and (d) *d*-wave. The corresponding angular dependences of the gaps are shown as the insets.

also reported in Refs. 6, 8, 16, 21, and 22. Bearing this in mind the data in Fig. 3 were analyzed by using single-gap and two-gap models, assuming that the superconducting energy gaps have the following symmetries: (a) *s*-wave, (b) *s* +*s*-wave, (c) anisotropic *s*-wave, and (d) *d*-wave.

Temperature dependence of the magnetic penetration depth λ was calculated within the local (London) approximation ($\lambda \gg \xi$, ξ is the coherence length) by using the following functional form:[23,24]

$$\frac{\lambda^{-2}(T)}{\lambda^{-2}(0)} = 1 + \frac{1}{\pi}\int_0^{2\pi}\int_{\Delta(T,\varphi)}^{\infty}\left(\frac{\partial f}{\partial E}\right)\frac{EdEd\varphi}{\sqrt{E^2-\Delta(T,\varphi)^2}}. \quad (4)$$

Here $\lambda^{-2}(0)$ is the zero-temperature value of the magnetic penetration depth, $f=[1+\exp(E/k_BT)]^{-1}$ is the Fermi function, φ is the angle along the Fermi surface, and $\Delta(T,\varphi)=\Delta_0\delta(T/T_c)g(\varphi)$ (Δ_0 is the maximum gap value at $T=0$). The temperature dependence of the gap is approximated by $\delta(T/T_c)=\tanh\{1.82[1.018(T_c/T-1)]^{0.51}\}$.[25] The function $g(\varphi)$ describes the angular dependence of the gap and is given by $g^s(\varphi)=1$ for the *s*-wave gap, $g^d(\varphi)=|\cos(2\varphi)|$ for the *d*-wave gap, and $g^{s\mathrm{An}}(\varphi)=(1+a\cos 4\varphi)/(1+a)$ for the anisotropic *s*-wave gap.[26]

The two-gap calculations were performed within the framework of the so-called α model assuming that the total superfluid density is a sum of two components[24,25]

$$\frac{\lambda^{-2}(T)}{\lambda^{-2}(0)} = \omega\cdot\frac{\lambda^{-2}(T,\Delta_{0,1})}{\lambda^{-2}(0,\Delta_{0,1})} + (1-\omega)\cdot\frac{\lambda^{-2}(T,\Delta_{0,2})}{\lambda^{-2}(0,\Delta_{0,2})}. \quad (5)$$

Here $\Delta_{0,1}$ and $\Delta_{0,2}$ are the zero-temperature values of the large and the small gaps, respectively, and ω ($0\leq\omega\leq1$) is the weighting factor which represents the relative contribution of the larger gap to λ^{-2}.

The results of the analysis are presented in Fig. 3 by solid black lines. The angular dependences of the gaps $[\Delta_0\cdot g(\varphi)]$ are shown as insets. The goodness of fit was tested using the χ^2 criterion. The values of χ^2 normalized to the number of degrees of freedom minus 1 (χ^2_{norm}) are presented in the corresponding graphs. It is obvious that the simple *s*-wave approach cannot describe the observed $\lambda_{ab}^{-2}(T)$ [see Fig. 3(a)]. The fit by using *d*-wave model results in $\chi_{\mathrm{norm}}\simeq1.73$ which is bigger than that obtained within the framework of anisotropic *s*- and *s*+*s*-wave models. The constant, within our experimental uncertainty, $\lambda_{ab}^{-2}(T)$ at $T\lesssim1$ K is also inconsistent with the presence of any type of nodes in the energy gap of $FeSe_{0.85}$. In contrast, both anisotropic *s*- and two-gap *s* +*s*-wave models [Figs. 3(b) and 3(c)] describe the experimental data reasonably well. It should be noted, however, that the fit within the anisotropic *s*-wave model results in $\simeq$10% smaller value of χ^2_{norm}. In the following we are going to discuss separately the results obtained within the framework of these two models. For the anisotropic *s*-wave case we get $\Delta_0=2.24(1)$ meV, $a=0.798(6)$, and $\lambda_{ab}(0)=406(5)$ nm. The corresponding gap to T_c ratio is $2\Delta_0/k_BT_c=6.27(3)$ close to that reported in Ref. 18 for $NdFeAsO_{0.9}F_{0.1}$. The obtained variation with angle $\Delta^{\max}/\Delta^{\min}=2.24/0.252\simeq8.9$ is, however, substantially bigger than 1.2 reported in.[18,19] The fit within the two-gap *s*+*s*-wave model yields $\Delta_{0,1}=1.60(2)$ meV, $\Delta_{0,2}=0.38(1)$ meV, $\omega=0.658(5)$, and $\lambda_{ab}(0)=404(5)$ nm. The "large" and the "small" gap to T_c ratios $2\Delta_{0,1}/k_BT_c=4.49(6)$ and $2\Delta_{0,2}/k_BT_c=1.07(2)$ are close to those reported for various single- and double-layer pnictide superconductors based on the results of the point contact Andreev reflection spectroscopy experiments of Szabo *et al.*[6] and Gonelli *et al.*[7] and the first critical field measurements of Ren *et al.*[8] The multiple gaps may originate from the multiple bands at the Fermi level of $FeSe_{0.85}$. First-principles calculation indicates that the Fermi surface (FS) of FeSe is quasi-two-dimensional and consists of hole-type sheets around the Γ point and electron-type sheets around the M point of the Brillouin zone.[27] It is conceivable that the two gaps open up on the different sheets of the FS. In this context, the present compound may resemble the situation of MgB_2 where a large gap opens on the FS derived from the orbitals in the boron plane, while a small gap opens on the FS derived from orbitals perpendicular to the boron plane.[28]

To conclude, muon-spin-rotation measurements were performed on the superconductor $FeSe_{0.85}$ ($T_c \simeq 8.3$ K). $\lambda_{ab}^{-2}(T)$ was reconstructed from the temperature dependence of the Gaussian muon depolarization rate measured at $\mu_0 H = 0.01$ T. The absolute value of the in-plane magnetic penetration depth λ_{ab} at $T=0$ was estimated to be $\lambda_{ab}(0) = 405(7)$ nm. The temperature dependence of λ_{ab}^{-2} was found to be inconsistent with an isotropic s-wave symmetry of the superconducting energy gap. A good agreement between the experimental data and the theory was obtained within the framework of two-gap $s+s$ and anisotropic s-wave gap models, thus suggesting that the superconducting energy gap in $FeSe_{0.85}$ superconductor is fully developed and contains no nodes.

This work was performed at the Swiss Muon Source (SμS), Paul Scherrer Institute (PSI, Switzerland). The work was partly supported by the NCCR program MaNEP.

*rustem.khasanov@psi.chf

[1] Y. Kamihara *et al.*, J. Am. Chem. Soc. **130**, 3296 (2008).
[2] C. Wang *et al.*, Europhys. Lett. **83**, 67006 (2008); Z.-A. Ren *et al.*, *ibid.* **83**, 17002 (2008); A. S. Sefat *et al.*, Phys. Rev. B **77**, 174503 (2008); G. F. Chen *et al.*, Phys. Rev. Lett. **100**, 247002 (2008); H. Wen *et al.*, Europhys. Lett. **82**, 17009 (2008); J. Yang *et al.*, arXiv:0809.3582 (unpublished).
[3] M. Rotter *et al.*, Phys. Rev. B **78**, 020503(R) (2008); M. Rotter *et al.*, Phys. Rev. Lett. **101**, 107006 (2008); Gen-Fu Chen *et al.*, Chin. Phys. Lett. **25**, 3403 (2008); N. Ni *et al.*, Phys. Rev. B **78**, 014523 (2008); M. S. Torikachvili *et al.*, Phys. Rev. Lett. **101**, 057006 (2008).
[4] G. Wu *et al.*, Phys. Rev. B **78**, 092503 (2008); M. J. Pitcher *et al.*, Chem. Commun. (Cambridge) **2008**, 5819; J. H. Tapp *et al.*, Phys. Rev. B **78**, 060505(R) (2008).
[5] F.-C. Hsu *et al.*, Proc. Natl. Acad. Sci. U.S.A. **105**, 14262 (2008).
[6] P. Szabo *et al.*, arXiv:0809.1566 (unpublished).
[7] R. S. Gonnelli *et al.*, arXiv:0807.3149 (unpublished).
[8] C. Ren *et al.*, arXiv:0808.0805 (unpublished).
[9] R. Khasanov *et al.*, Phys. Rev. B **78**, 092506 (2008).
[10] R. E. Walstedt and L. R. Walker, Phys. Rev. B **9**, 4857 (1974).
[11] A. Schenck, *Muon Spin Rotation: Principles and Applications in Solid State Physics* (Adam Hilger, Bristol, 1986).
[12] P. Zimmermann *et al.*, Phys. Rev. B **52**, 541 (1995).
[13] V. I. Fesenko, V. N. Gorbunov, and V. P. Smilga, Physica C **176**, 551 (1991).
[14] H. Schilling *et al.*, J. Phys. F: Met. Phys. **12**, 875 (1982).
[15] E. H. Brandt, Phys. Rev. B **37**, 2349 (1988).
[16] H. Ding *et al.*, Europhys. Lett. **83**, 47001 (2008).
[17] T. Y. Chen *et al.*, Nature (London) **453**, 1224 (2008); K. Hashimoto *et al.*, arXiv:0806.3149 (unpublished).
[18] T. Kondo *et al.*, Phys. Rev. Lett. **101**, 147003 (2008).
[19] C. Martin *et al.*, arXiv:0807.0876 (unpublished).
[20] M. C. Boyer *et al.*, arXiv:0806.4400 (unpublished); C. Ren *et al.*, arXiv:0804.1726 (unpublished); L. Shan *et al.*, Europhys. Lett. **83**, 57004 (2008); H.-J. Grafe *et al.*, Phys. Rev. Lett. **101**, 047003 (2008); Y. Nakai *et al.*, J. Phys. Soc. Jpn. **77**, 073701 (2008); H. Mukuda *et al.*, *ibid.* **77**, 093704 (2008); H. Kotegawa *et al.*, *ibid.* **77**, 113703 (2008).
[21] L. Malone *et al.*, arXiv:0806.3908 (unpublished).
[22] D. V. Evtushinsky *et al.*, arXiv:0809.4455 (unpublished).
[23] M. Tinkham, *Introduction to Superconductivity* (Krieger, Malabar, Florida, 1975).
[24] R. Khasanov *et al.*, Phys. Rev. Lett. **98**, 057007 (2007).
[25] A. Carrington and F. Manzano, Physica C **385**, 205 (2003).
[26] L. Shan *et al.*, Phys. Rev. B **72**, 144506 (2005).
[27] A. Subedi *et al.*, Phys. Rev. B **78**, 134514 (2008).
[28] H. J. Choi *et al.*, Nature (London) **418**, 758 (2002).